

9. Jeevaratnam, J., Glasser, F. P. & Glasser, L. S. D. Anion substitution and structure of $12\text{CaO}\cdot 7\text{Al}_2\text{O}_3$. *J. Am. Ceram. Soc.* **47**, 105–106 (1964).
10. Hosono, H. & Abe, Y. Occurrence of superoxide radical ion in crystalline $12\text{CaO}\cdot 7\text{Al}_2\text{O}_3$ prepared via solid-state reaction. *Inorg. Chem.* **26**, 1192–1195 (1987).
11. Hayashi, K., Hirano, M., Matsuishi, S. & Hosono, H. Microporous crystal $12\text{CaO}\cdot 7\text{Al}_2\text{O}_3$ encaging abundant O^- radicals. *J. Am. Chem. Soc.* **124**, 738–739 (2002).
12. Watauchi, S., Tanaka, I., Hayashi, K., Hirano, M. & Hosono, H. Crystal growth of $\text{Ca}_{12}\text{Al}_{14}\text{O}_{33}$ by the floating zone method. *J. Cryst. Growth* **237**, 496–502 (2002).
13. Li, Q.-X. *et al.* Absolute emission current density of O^- from $12\text{CaO}\cdot 7\text{Al}_2\text{O}_3$. *Appl. Phys. Lett.* **80**, 4259–4261 (2002).
14. Henderson, B. & Wertz, J. E. Defects in the alkaline earth oxides. *Adv. Phys.* **17**, 749–855 (1968).
15. Agullo-Lopez, F., Catlow, C. R. A. & Townsend, P. D. *Point Defects in Materials* Ch. 5 (Academic, London, 1988).
16. Williams, R. T. & Friebele, E. J. *CRC Handbook of Laser Science and Technology* (ed. Weber, M. J.) Part I Vol. III (CRC, Boca Raton, FL, 1986).
17. Hosono, H., Asada, N. & Abe, Y. Properties and mechanism of photochromism in reduced calcium aluminate glasses. *J. Appl. Phys.* **67**, 2840–2847 (1990).
18. Giamello, E., Paganini, M. C., Murphy, D. M., Ferrari, A. M. & Pacchioni, G. A. Combined EPR and quantum chemical approach to the structure of surface F_2^+ (H) centres on MgO. *J. Phys. Chem.* **101**, 971–982 (1997).
19. Oliver, D., Hofmann, P. & Knözinger, E. H_2 chemisorption and consecutive uv stimulated surface reactions on nanostructured MgO. *Phys. Chem. Chem. Phys.* **1**, 713–721 (1999).
20. Hayward, M. A. *et al.* The hydride anion in an extended transition metal oxide array: $\text{LaSrCoO}_3\text{H}_{0.7}$. *Science* **295**, 1882–1884 (2002).
21. Mott, N. F. & Davis, E. A. *Electronic Processes in Non-crystalline Materials*, 2nd edn (Oxford Univ. Press, Oxford, 1979).
22. Weil, J. A., Bolton, J. R. & Wertz, J. E. *Electron Paramagnetic Resonance* (Wiley, 1994).

Acknowledgements

We thank I. Tanaka and S. Watauchi for growing the single crystals, S. Takeda for NMR measurements, and M. Sadakata, Q.-X. Li and T. Nishioka for TOF-MS measurements.

Competing interests statement

The authors declare that they have no competing financial interests.

Correspondence or requests for materials should be addressed to K.H. (e-mail: k-hayashi@net.ksp.or.jp).

Switch of flow direction in an Antarctic ice stream

H. Conway*, G. Catania*, C. F. Raymond*, A. M. Gades*, T. A. Scambos† & H. Engelhardt‡

* Earth and Space Sciences, University of Washington, Seattle, Washington 98195, USA

† National Snow and Ice Data Center, University of Colorado, Boulder, Colorado 80309, USA

‡ Geological and Planetary Sciences, California Institute of Technology, Pasadena, California 99125, USA

Fast-flowing ice streams transport ice from the interior of West Antarctica to the ocean, and fluctuations in their activity control the mass balance of the ice sheet. The mass balance of the Ross Sea sector of the West Antarctic ice sheet is now positive—that is, it is growing—mainly because one of the ice streams (ice stream C) slowed down about 150 years ago¹. Here we present evidence from both surface measurements and remote sensing that demonstrates the highly dynamic nature of the Ross drainage system. We show that the flow in an area that once discharged into ice stream C has changed direction, now draining into the Whillans ice stream (formerly ice stream B). This switch in flow direction is a result of continuing thinning of the Whillans ice stream and recent thickening of ice stream C. Further abrupt reorganization of the activity and configuration of the ice streams over short timescales is to be expected in the future as the surface topography of the ice sheet responds to the combined effects of internal dynamics and long-term climate change. We suggest that

caution is needed when using observations of short-term mass changes to draw conclusions about the large-scale mass balance of the ice sheet.

Both the volume and areal extent of the West Antarctic ice sheet have decreased greatly since the early Holocene epoch^{2–4}, and there is debate about its future, partly because of its potentially large effect on global sea level^{5–7}. The grounding line in the Ross Sea sector has on average retreated at about 120 m yr^{-1} for at least 7,500 years; at this rate, complete deglaciation of the Ross Sea sector will take about 7,000 years (ref. 7). However, recent calculations based on synthetic aperture radar altimetry indicate overall growth of the Ross drainage system¹. It is unclear whether the present growth, which began less than two centuries ago, is due to unsteady flow of the ice streams, or if it signals the end of the Holocene retreat.

Fast-flowing ice streams dominate the modern drainage system of West Antarctica. Fast flow is enabled through lubrication of the bed by pressurized water and weak subglacial till^{8,9}, which allows rapid motion (10^2 to 10^3 m yr^{-1}) in spite of the very low surface slopes and associated low gravitational driving stress^{10,11}. The widths of the Ross ice streams are constrained by relatively stable ridges of slow-moving ice (Fig. 1), and spectacular zones of chaotic crevasses form¹² at the lateral margins of ice streams that are flowing faster than about 100 m yr^{-1} . Emerging evidence of former (now buried) shear margins and other relict flow features show that the configuration and activity of the Ross ice stream system has undergone major reorganization in the recent past; Siple ice stream stagnated 450 years ago (ref. 13; and B. E. Smith, unpublished results); the lower reaches of ice stream C (ISC) stagnated 150 years ago¹⁴; the Whillans ice stream (WIS) is now slowing and migrating^{15–17}. Such changes are indicative of a highly dynamic drainage system that is reminiscent of braided stream systems, which as a whole can be relatively stable even as individual channels exhibit rapid reorganization over short timescales^{18,19}.

Flow stripes and surface morphology similar to those seen on active ice streams^{11,15} are visible in the image of the eastern end of

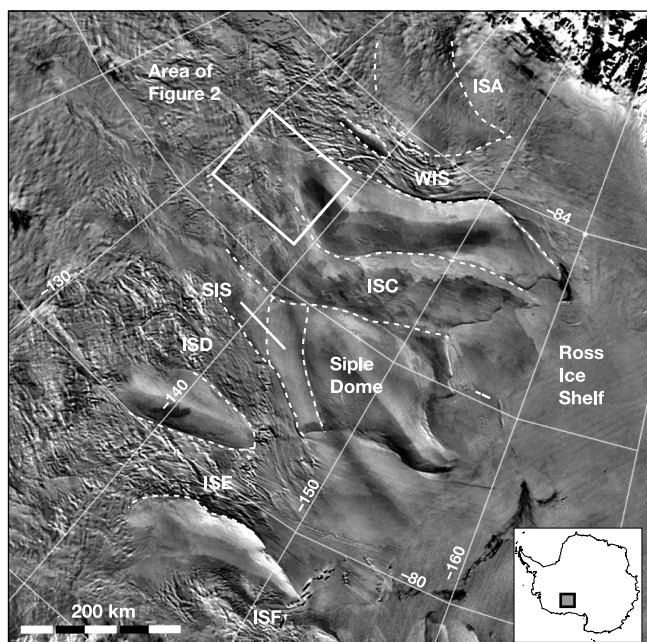


Figure 1 Satellite image of the Ross Sea ice drainage system in West Antarctica. White dashed lines delineate the lateral margins of present and former ice streams. The active ice streams (Whillans ice stream; WIS; ice streams A, D, E, F; ISA, ISD, ISE, ISF) flow at speeds up to 800 m yr^{-1} . Siple ice stream (SIS) stopped streaming 450 years ago (ref. 13; and B. E. Smith, unpublished results) and the lower reaches of ice stream C (ISC) stagnated about 150 years ago¹⁴.

Ridge BC (Fig. 2). Our ground-based radar profiles (Fig. 3) confirm the impression that ice once streamed across the ridge. The disturbed internal layering and diffractors, which are the tops of buried crevasses¹⁷, indicate that streaming flow (faster than about 100 m yr^{-1}) with associated high rates of marginal shearing has occurred in the past¹². We calculate the time of slowdown by tracking the deepest undisturbed radar layer across the top of the buried crevasses to a nearby core where the age–depth relationship has been measured²⁰. Results indicate that streaming flow ceased about 250 years ago, which is 100 years before the lower reaches of ISC stagnated, but 200 years after Siple ice stream stopped.

The elevation of the northern tributary of Whillans ice stream (WIS2) is now 120 m lower than ISC1 (a tributary of ISC), but the direction of past flow must have been toward the north into ISC for several reasons. (1) Analysis of the pattern of radar-detected internal layers across Ridge BC has shown that WIS2 has thinned about 200 m relative to ISC1 over the past 1,000 years (ref. 21). (2) The upper reaches of WIS2 are thinning²² and if the present rate (0.6 to 0.8 m yr^{-1}) has persisted since 250 years ago, it would have been 150–200 m higher then. ISC1 has thickened about 50 m since it stagnated²³, and so by this analysis WIS2 would have been 80–130 m higher than ISC1 250 years ago. Long-term thinning at half the present rate would still place WIS2 higher than ISC1 250 years ago. (3) The regional flow of ice is toward the northwest¹. Hence, we infer that this flow-path used to be a tributary to ISC, and because of its location to the south of tributary ISC1 (previously thought to be the

southern-most tributary of ISC) we name it ice stream C0 (ISC0).

Our measurements of surface velocity show that ice now flows southward out of ISC1 toward WIS2 (Fig. 2), which is almost completely opposite to the direction of past flow. The present-day flow, which cuts across the relict margin of ISC1 and other visible flow stripes (Fig. 2), follows closely the direction of surface slope. Observations suggest the following sequence of events: (1) about 1,000 years ago WIS2 started to thin faster than ISC for some reason that is unknown; (2) about 250 years ago thinning and inland migration of WIS2 beheaded tributary ISC0 and caused it to stagnate; (3) continuing thinning of WIS2 and more recent thickening of ISC1 has subsequently altered the surface topography in a way that has reversed the direction of both the gravitational driving

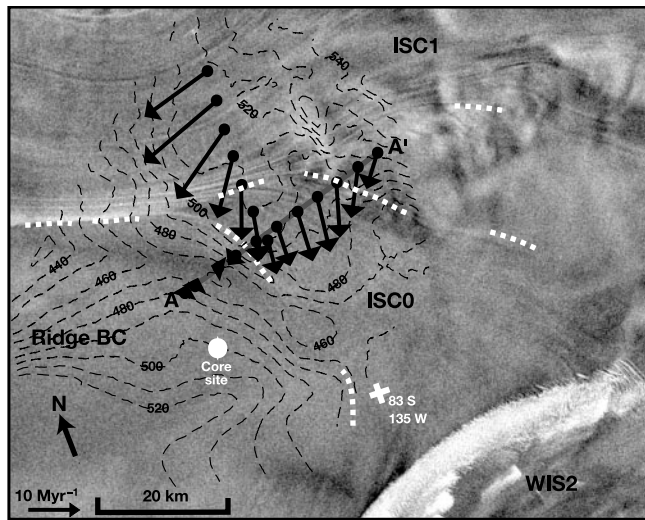


Figure 2 Flow features at the eastern end of Ridge BC (location shown in Fig. 1). The underlying image is derived from synthetic aperture radar data from the Radarsat Antarctic Mapping Mission (AMM-1) mosaic²⁸. Bright band at lower right is a result of scattering from open crevasses at the margin of the northern tributary of the Whillans ice stream (WIS2). Flow stripes, which are often visible on fast-flowing ice streams¹⁵, are also visible on the formerly active tributaries of ice stream C (ISC1 and ISC0). Black dashed lines, elevation contours (metres above WGS84) derived from GPS measurements and photogrammetry²⁹. White dashed lines, relict ice stream margins inferred from buried crevasses that have been detected by others¹³ and by us using ice-penetrating radar. A–A', the location of the radar traverse shown in Fig. 3. The measured accumulation rate at the core site²⁰ is 8.8 cm yr^{-1} (ice equivalent). Crevasse tops are about 18 m below the surface along the southern margin of ISC1, which corresponds to an age of ~ 150 yrs before present, BP. Crevasses on the newly discovered tributary ISC0 are now buried 28 m below the surface (corresponding age is 250 yr BP). Present-day surface velocities (represented by arrows) were calculated from repeat GPS surveys (up to 13 months between surveys) of poles placed in the snow. The modern flow cuts across visible flow stripes; apparently the motion in the new direction has not yet been sufficient to deform the flow stripes significantly.

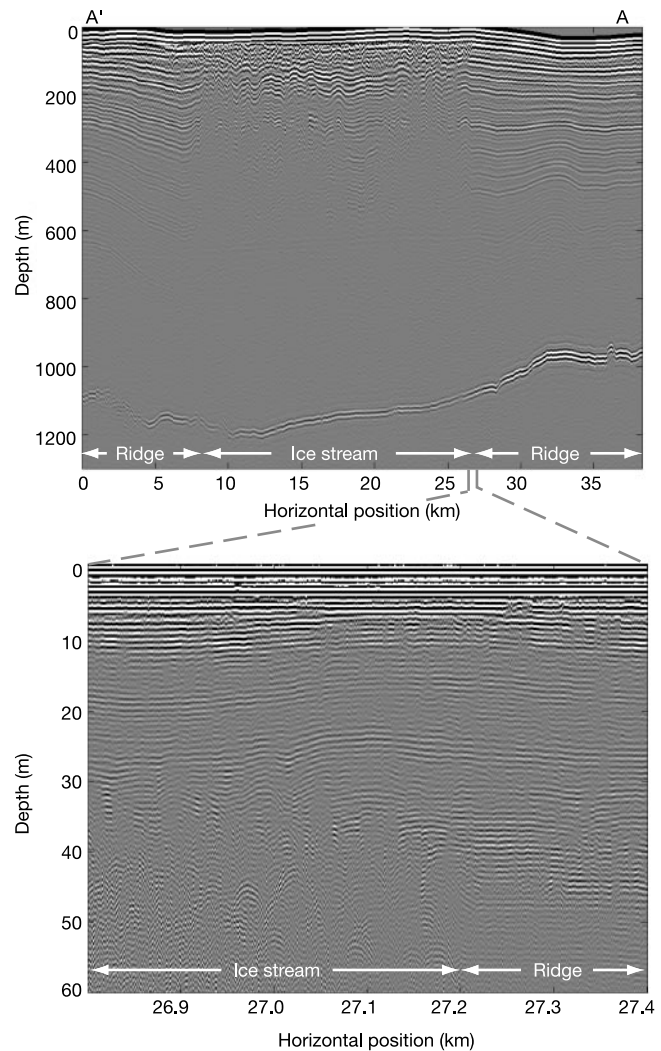


Figure 3 Ice-penetrating radar profiles along A–A' in Fig. 2. Present-day flow direction is into the page. Top, low-frequency (5 MHz) radar profile starts at $82.68^\circ \text{ S } 134.33^\circ \text{ W}$ and ends on Ridge BC. The upper 40 m are not resolved by the system. The bright reflector near 1,100 m is the bed. Internal layers on the ridges at both ends of the profile (visible to depths of 700 m) are continuous and relatively undisturbed. The disturbed internal layers between 6.5 km and 27.22 km are typical of those observed within active ice streams. Bottom, high-frequency (100 MHz) measurements show near-surface details of the transition across the western margin of the former ice stream. With this system the upper 5 m are not resolved, but outside the limits of the former ice stream (27.22 to 27.4 km), continuous internal layers are visible to depths greater than 60 m. Diffractors, visible between 26.8 and 27.2 km within the ice stream, are the tops of buried crevasses, indicating that high rates of strain have occurred in the past¹². The deepest undisturbed layer across the tops of the buried crevasses is 28 m below the surface.

stress and the flow of sub-glacial water (the basal hydraulic gradient is controlled primarily by the surface slope²⁴). This likely sequence of events raises the possibility that the shutdown of flow of ice and basal water through ISCO contributed to the eventual stagnation of the trunk region of ice stream C about 100 years later. Others have also suggested that the slow-down of ISC was a result of re-routing of ice²⁵ or basal water²⁶ away from the main trunk of the ice stream.

Of particular consequence are implications for the future. On the basis of the present-day geometry (ice thickness about 1.1 km, surface slope about 1.8×10^{-3}), measured surface velocities toward WIS2 (up to 20 m yr^{-1}) are two orders of magnitude faster than those expected from deformation of the ice column alone²⁷. Most of the speed today is a result of basal motion, which is not surprising because fast flow requires a lubricated bed, and liquid water has been detected in boreholes that have been drilled to the bed in the region⁸. Basal meltwater production will increase if flow continues to accelerate¹⁰, which could lead to streaming velocities in the near future. The mass balance of the Ross ice streams is now positive¹, but flow of 600 m yr^{-1} through such a hypothetical tributary (WIS3—1.1 km thick and 30 km wide) would discharge about $20 \times 10^{12} \text{ kg yr}^{-1}$ and effectively eliminate the present imbalance not only of ISC, but also of the entire Ross drainage system. □

Received 12 June; accepted 22 August 2002; doi:10.1038/nature01081.

1. Joughin, I. & Tulacz, S. Positive mass balance of the Ross Ice Streams, West Antarctica. *Science* **295**, 476–480 (2002).
2. Denton, G. H. & Hughes, T. J. Reconstructing the Antarctic Ice Sheet at the Last Glacial Maximum. *Quat. Sci. Rev.* **21**, 193–202 (2002).
3. Shipp, S., Anderson, J. & Domack, E. Late Pleistocene-Holocene retreat of the West Antarctic ice-sheet system in the Ross Sea: Part 1 – Geophysical results. *Geol. Soc. Am. Bull.* **111**, 1486–1516 (1999).
4. Conway, H., Hall, B. L., Denton, G. H., Gades, A. M. & Waddington, E. D. Past and future grounding-line retreat of the West Antarctic Ice Sheet. *Science* **286**, 280–283 (1999).
5. Bentley, C. R. West Antarctic Ice Sheet collapse? *Science* **276**, 663–664 (1997).
6. Oppenheimer, M. Global warming and the stability of the West Antarctic Ice Sheet. *Nature* **393**, 325–332 (1998).
7. Bindschadler, R. A. Future of the West Antarctic Ice Sheet. *Science* **282**, 428–429 (1998).
8. Kamb, B. in *The West Antarctic Ice Sheet: Behavior and Environment* (eds Alley, R. B. & Bindschadler, R. A.) Antarctic Research Series 77 157–199 (American Geophysical Union, Washington DC, 2001).
9. Tulacz, S., Kamb, B. & Engelhardt, H. Basal mechanics of Ice Stream B, West Antarctica 2. Undrained plastic bed model. *J. Geophys. Res.* **105**, 483–494 (2000).
10. Raymond, C. F. Energy balance of ice streams. *J. Glaciol.* **46**, 665–674 (2000).
11. Whillans, I. M., Bentley, C. R. & van der Veen, C. J. in *The West Antarctic Ice Sheet: Behavior and Environment* (eds Alley, R. B. & Bindschadler, R. A.) Antarctic Research Series 77 257–281 (American Geophysical Union, Washington DC, 2001).
12. Vaughan, D. G. Relating the occurrence of crevasses to surface strain rates. *J. Glaciol.* **39**, 255–266 (1993).
13. Jacobel, R. W., Scambos, T. A., Nereson, N. A. & Raymond, C. F. Changes in the margin of Ice Stream C, Antarctica. *J. Glaciol.* **46**, 102–110 (2000).
14. Retzlaff, R. & Bentley, C. R. Timing of stagnation of Ice Stream C, West Antarctica from short-pulse-radar studies of buried crevasses. *J. Glaciol.* **39**, 553–561 (1993).
15. Fahnestock, M. A., Scambos, T. A., Bindschadler, R. A. & Kvaran, G. A millennium of variable ice-flow recorded by the Ross Ice Shelf, Antarctica. *J. Glaciol.* **46**, 652–664 (2000).
16. Bindschadler, R. & Vornberger, P. Changes in the West Antarctic Ice Sheet since 1963 from declassified satellite photography. *Science* **279**, 689–692 (1998).
17. Clarke, T. S., Liu, C., Lord, N. E. & Bentley, C. R. Evidence for a recently abandoned shear margin adjacent to Ice Stream B2, Antarctica, from ice-penetrating radar measurements. *J. Geophys. Res.* **105**, 13409–13422 (2000).
18. Catania, G. & Paola, C. Braiding under glass. *Geology* **29**, 259–262 (2001).
19. Murray, A. B. & Paola, C. A cellular model of braided rivers. *Nature* **371**, 54–57 (1994).
20. Alley, R. B. & Bentley, C. R. Ice-core analysis on the Siple Coast of West Antarctica. *Ann. Glaciol.* **11**, 1–7 (1988).
21. Nereson, N. A. & Raymond, C. F. The elevation history of ice streams and the spatial accumulation pattern along the Siple Coast of West Antarctica inferred from ground-based radar data from three inter-ice-stream ridges. *J. Glaciol.* **47**, 303–313 (2001).
22. Shabtaie, S., Bentley, C. R., Bindschadler, R. A. & MacAyeal, D. R. Mass-balance studies of Ice Streams A, B and C, West Antarctica, and possible surging behavior of Ice Stream B. *Ann. Glaciol.* **11**, 165–172 (1988).
23. Price, S. F., Bindschadler, R. A., Hulbe, C. L. & Joughin, I. R. Post-stagnation behavior in the upstream regions of Ice Stream C, West Antarctica. *J. Glaciol.* **47**, 283–294 (2001).
24. Weertman, J. General theory of water flow at the base of a glacier or ice sheet. *Rev. Geophys. Space Phys.* **10**, 287–333 (1972).
25. Rose, K. E. Characteristics of ice flow in Marie Byrd Land, Antarctica. *J. Glaciol.* **24**, 63–74 (1979).
26. Anandakrishnan, S. & Alley, R. B. Stagnation of Ice Stream C, West Antarctica by water piracy. *Geophys. Res. Lett.* **24**, 265–268 (1997).
27. Paterson, W. S. B. *The Physics of Glaciers* (Pergamon, Oxford, 1994).
28. Jezek, K. C. Glaciological properties of the Antarctic ice sheet from RADARSAT-1 synthetic aperture imagery. *Ann. Glaciol.* **27**, 33–40 (1999).
29. Scambos, T. A. & Fahnestock, M. A. Improving digital elevation models over ice sheets using AVHRR-based photoclinometry. *J. Glaciol.* **44**, 97–103 (1998).

Acknowledgements

We thank Raytheon Polar Services for logistical support in Antarctica, and C. R. Bentley, M. Conway, N. Lord and B. Smith for contributions. This work was supported by the US National Science Foundation.

Competing interests statement

The authors declare that they have no competing financial interests.

Correspondence and requests for materials should be addressed to H.C.

(e-mail: conway@ess.washington.edu).

Lateralization of magnetic compass orientation in a migratory bird

Wolfgang Wiltschko*, Joachim Traudt*, Onur Güntürkün†, Helmut Prior† & Roswitha Wiltschko*

* Zoologisches Institut, Fachbereich Biologie und Informatik, J.W. Goethe-Universität, Siesmayerstrasse 70, D-60054 Frankfurt am Main, Germany

† AE Biopsychologie, Fakultät für Psychologie, Ruhr-Universität Bochum, D-44780 Bochum, Germany

Lateralization of brain functions, once believed to be a human characteristic, has now been found to be widespread among vertebrates^{1–3}. In birds, asymmetries of visual functions are well studied, with each hemisphere being specialized for different tasks^{4–8}. Here we report lateralized functions of the birds' visual system associated with magnetoperception, resulting in an extreme asymmetry of sensing the direction of the magnetic field. We found that captive migrants tested in cages with the magnetic field as the only available orientation cue were well oriented in their appropriate migratory direction when using their right eye only, but failed to show a significant directional preference when using their left eye. This implies that magnetoreception for compass orientation, assumed to take place in the eyes alongside the visual processes^{9–11}, is strongly lateralized, with a marked dominance of the right eye/left brain hemisphere.

In birds, fibres of the optic nerves cross over completely and interhemispheric commissures are comparatively small. As a consequence, visual input from the right eye is predominantly processed by the left hemisphere and vice versa. Studies testing monocular birds with one eye occluded suggest a division of functions between the two hemispheres, with the left eye/right hemisphere being specialized for geometric aspects of visual cues and novelty⁸, whereas the right eye/left hemisphere predominantly processes object vision^{5,6,12}. These studies concerned tests performed in the small-scale surroundings of laboratories. However, recent studies with pigeons homing over distances of up to 40 km revealed that monocular birds using their right eye performed



Figure 1 A robin ready for monocular testing. Left, view of the covered eye; right, view of the open eye. J.T. took the photographs.